JOURNAL OF GEOPHYSICAL RESEARCH, VOL. 99, NO. B12, PAGES 24,121–24,134, DECEMBER 10, 1994

Skewness of marine magnetic anomalies created between 85 and 40 Ma in the Indian Ocean

J. Dyment[1]

Earth and Planetary Sciences, McGill University, Montréal, Québec, Canada

S.C. Cande

Scripps Institution of Oceanography, La Jolla, California

J. Arkani-Hamed

Earth and Planetary Sciences, McGill University, Montréal, Québec, Canada

Abstract. We have performed a detailed analysis of the skewness of marine magnetic anomalies in Indian Ocean basins created between 85 and 40 Ma as a result of the northward motion of India. Visual and semiautomated methods of skewness determination were applied to the data. Both provide consistent results, but the visual method is prefered for its ability to deal with noisy data. Plots of apparent effective remanent inclination (or skewness corrected for present geomagnetic field inclination) versus time for conjugate basins display the combination of three effects: a gradual increase with time, related to the northward motion of the ridges attached to India in the geomagnetic reference frame; a gap between conjugate curves, which represents anomalous skewness senso stricto; and short-period fluctuations, which represent the sequence effect, i.e., the effect of neighboring magnetic sources on the skewness of a given anomaly. The anomalous skewness decreases with faster spreading rate and completely disappears above 50 km/m.y., an observation which negates geomagnetic field behavior as a possible cause of the observed anomalous skewness.

Introduction

Seafloor spreading marine magnetic anomalies exhibit a phase, or skewness, which depends on the inclination of both the magnetization and geomagnetic field vectors. Skewness measurements may therefore provide a tool to determine paleolatitudes [e.g., *McKenzie and Sclater,* 1971; *Schlich,* 1982] and paleomagnetic poles [*Schouten and Cande,* 1976; *Cande,* 1976; *Petronotis et al.,* 1992]. However, skewness analyses of magnetic anomalies from a worldwide distribution of conjugate basins (between Australia and Antarctica [*Weissel and Hayes,* 1972], across the Pacific-Antarctic Ridge [*Cande,* 1976], across the Mid-Atlantic Ridge [*Cande and Kristoffersen,* 1977; *Cande,* 1978; *Roest et al.,* 1992], in the Agulhas Basin [*LaBrecque and Hayes,* 1979], and in the Philippine Basin [*Watts et al.,* 1977; *Hilde and Lee,* 1984]) have demonstrated the existence of a residual component, named anomalous skewness [*Cande,* 1976], which may be as large as 50°. Anomalous skewness arises because the conventional assumption of rectangular, two-dimensional layer 2A prisms of constant magnetization and alternating polarity is only a first-order representation of the oceanic crustal magnetic source, which is suitable to build synthetics in order to identify anomalies for plate tectonic studies but is not adequate for a detailed analysis of the magnetic anomaly signal.

Very few skewness determinations have been made on Indian Ocean magnetic anomalies, as part of a more general study by *Roest et al.* [1992]. This is unfortunate, as the Indian Ocean is probably one of the most suitable locations for the study of marine magnetic anomaly skewness. Compared to the Atlantic Ocean, which encountered only slow spreading rates, the Indian Ocean was characterized by a wide range of spreading rates during the last 100 m.y., from the ultra-slow Southwest Indian Ridge (6 km/m.y. half rate at anomalies 5-6, 10-20 Ma [*Patriat,* 1987]) to the ultra-fast Southeast Indian Ridge (105 km/m.y. half rate at anomalies 28-29, 65 Ma [*Patriat,* 1987]). In contrast to the Pacific Ocean, which is surrounded by subduction zones, the conjugate of most Indian Ocean basins still exists, the only exception being the northern Wharton Basin bounded by the Indonesian subduction zone (Figure 1).

[1]Also at URA 1278 et GDR GEDO, Université de Bretagne Occidentale, Brest, France.

Paper number 94JB02061.
0148-0227/94/94JB-02061$05.00

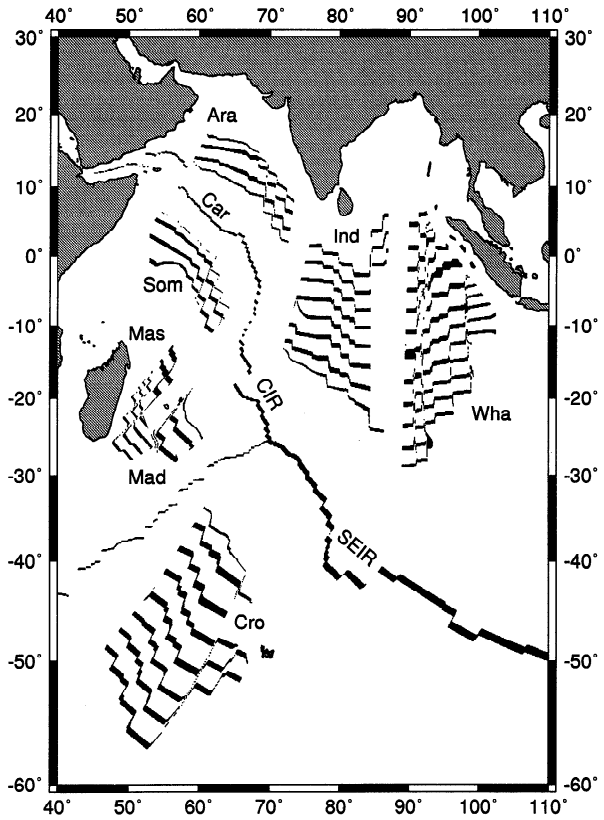

Figure 1a. Location of oceanic basins created as a result of the northward motion of India between 85 and 40 Ma. For this period, oceanic crust generated in 1 m.y. every 5 m.y. is shaded. The width and spacing of the resulting zebra patterns give a visual appreciation of relative spreading rates in the area. Ara, Arabian Basin; Cro, Crozet Basin; Ind, Central Indian Basin; Mad, Madagascar Basin; Mas, Mascarene Basin; Som, Eastern Somali Basin; Wha, Wharton Basin; Car, Carlsberg Ridge; CIR, Central Indian Ridge; SEIR, Southeast Indian Ridge.

In this paper, we use part of 3,000,000 km of marine magnetic anomaly data collected by various oceanographic institutions and gathered by the Indian Ocean Data Compilation Project to study the skewness of magnetic anomalies created between 85 and 40 Ma during the fast northward motion of India. This includes data from the Arabian, Eastern Somali, Mascarene, Madagascar, Central Indian, Crozet and Wharton basins (Figure 1).

Anomalous Skewness and Fossil Spreading Centers

Our interest in the Indian Ocean arises from the observation of strong anomalous skewness on profiles crossing fossil spreading centers in the Wharton Basin (Figure 2) and the Mascarene Basin, where the conjugate magnetic anomalies are very close and the effective inclination (i.e., the inclination along the spreading direction) of the present geomagnetic field varies by less than 5°. The effective inclination of magnetization is by definition the same for conjugate anomalies. These conjugate anomalies should therefore display the same skewness, and the application of a correct phase shift should produce symmetrical, boxlike anomalies on both flanks.

Attempts to deskew magnetic anomalies on each flank of the Wharton fossil spreading center (Figure 2, second and third profiles) show that this is obviously not the case: while all the anomalies of one flank are approximately symmetrical for a given phase shift, the anomalies of the other flank still display a strong asymmetry. Application of a mean phase shift (Figure 2, fourth profile) results in symmetrical magnetic anomalies with respect to the fossil spreading center; anomalies generally display a marked slope toward the fossil ridge axis. Assuming that anomalous skewness is evenly distributed between both flanks, the difference between phase shifts required to deskew the northern (Figure 2, second profile) and southern (Figure 2, third profile) flanks of this fossil spreading center is twice the anomalous skewness. The anomalous skewness reaches therefore about 30° in the Wharton Basin. Similarly, the anomalous skewness is about 20° in the Mascarene Basin.

Anomalous skewness has been observed in the vicinity of other fossil spreading centers. It reaches about 15° in the Philippine Basin for anomalies 13-24 [*Hilde*

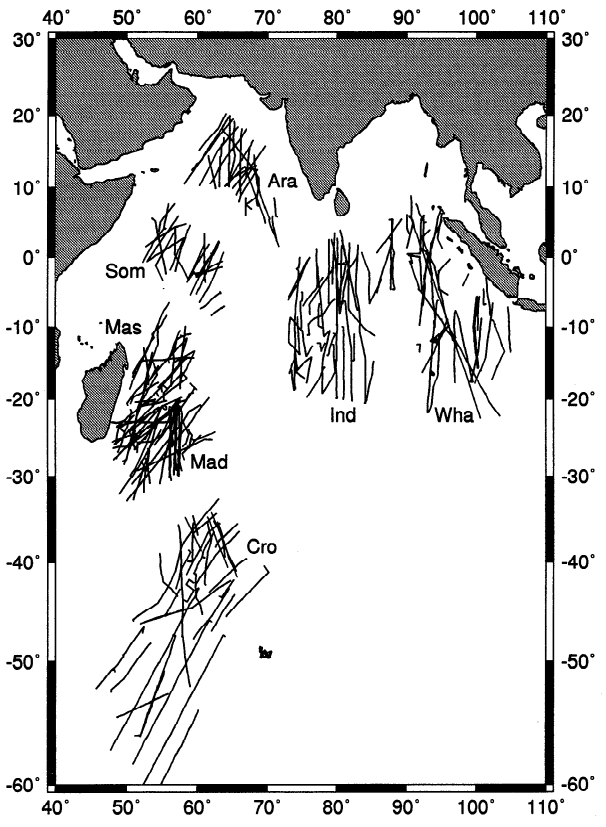

Figure 1b. Location of the shipborne magnetic anomaly profiles used in this study.

and Lee, 1984] and 30° in the Agulhas Basin for anomalies 33-34 [*LaBrecque and Hayes,* 1979]. The frequent association of anomalous skewness with fossil spreading centers may provide a clue for understanding the cause of anomalous skewness, although some fossil spreading centers were too slow (e.g., Labrador Sea [*Srivastava,* 1978], Norwegian Sea [*Talwani and Eldholm,* 1977]) or stopped after a period of very rapid geomagnetic reversals (e.g., South China Sea [*Briais et al.,* 1993], Somali Basin [*Cochran,* 1988]) to allow any reliable anomalous skewness observation.

Data Analysis

The determination of the skewness parameter of marine magnetic anomalies is not an easy task. Various criteria have been proposed for the deskewed magnetic anomalies. *LaBrecque* [1973, 1976], *Schouten and Cande* [1976], *Petronotis and Gordon* [1989], and *Arkani-Hamed* [1991] consider that a deskewed anomaly should be identical to the corresponding synthetic anomaly computed at the pole, i.e., with vertical magnetization and geomagnetic field vectors, assuming rectangular, two-dimensional prisms of constant magnetization and alternating polarity (criterion 1). In a simplified version of this criterion, a deskewed magnetic anomaly should be symmetrical, like the anomaly resulting from a single rectangular, two-dimensional prism of constant magnetization at the geomagnetic pole (criterion 2). *Roest et al.* [1992] assume that a deskewed anomaly should maximize the correlation between two functions derived from the anomaly, the modulus of the analytic signal and the horizontal derivative of the pseudo-gravity (criterion 3).

These criteria lead to similar but not identical results. To estimate the difference between results obtained by using criteria 1 and 2, we examine the phase shift required to produce symmetric individual synthetic anomalies computed at the pole using rectangular, two-dimensional prisms of constant magnetization and alternating polarity. Adopting the polarity timescale of *Cande and Kent* [1992] and the spreading rates considered hereafter, this phase shift represents typically less than 5° but may reach 12° for some anomalies at slow spreading rates. This phase shift is caused by neighboring sources because the magnetic anomaly created by a rectangular, two-dimensional prism of constant magnetization is symmetrical. It is therefore the result of an uneven distribution of the prisms and a combined effect of the geomagnetic polarity timescale and spreading rates.

Criterion 1 takes into account the effect of neighboring sources and, in a certain way, implies a partial deconvolution of the source function assuming a given sequence of rectangular, two dimensional prisms of constant magnetization. To be properly applied, it requires the computation of synthetics for every profile analyzed, as varying spreading rate, ridge jumps, assymetry, and complex segmentation affects the sequence of alternating polarities. We prefer, for simplicity, to adopt criterion 2 and consider that a magnetic anomaly is deskewed if it is symmetrical. In the case

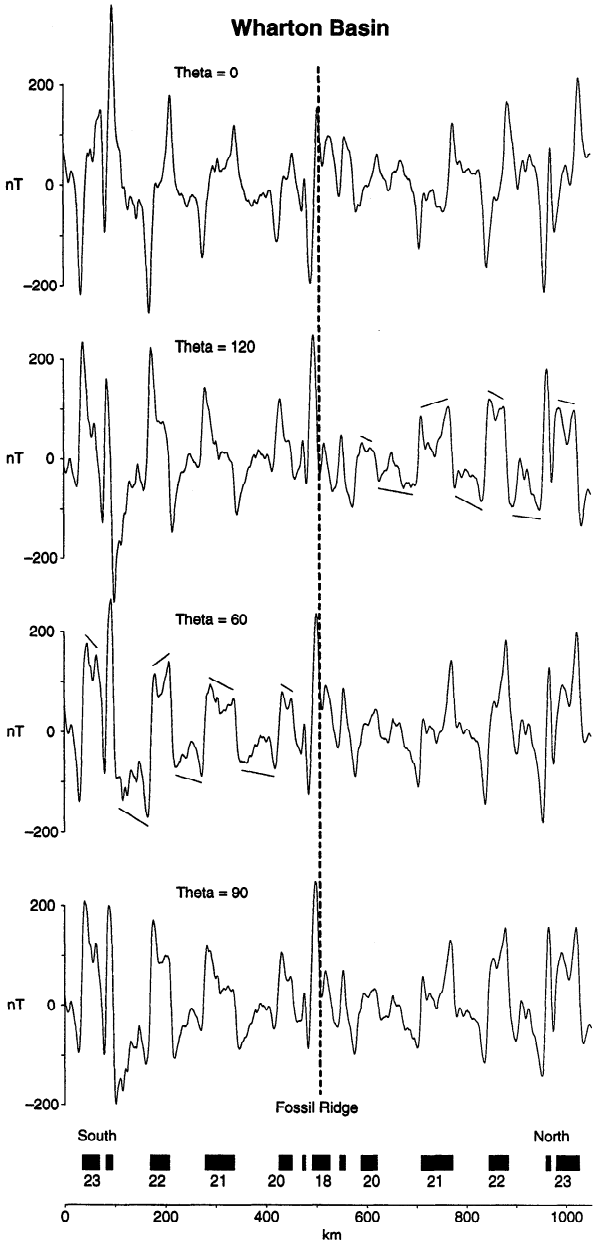

Figure 2. Magnetic anomaly profile across the Wharton Basin fossil spreading center (R/V *Jean Charcot* profile 03-16 [*Schlich et al.,* 1985]). From top to bottom, the initial data (Theta = 0) are phase-shifted to approximately deskew anomalies on the northern flank (Theta = 120°) and on the southern flank (Theta = 60°) as shown by line segments over the anomalies. The selected phase shifts are satisfactory for a group of anomaly (i.e., on a fossil ridge flank) and represent an average of the optimal phase shift for each individual anomaly. Later in this paper, we determine skewness for individual anomalies only. Average phase shift (Theta = 90°) results in a symmetrical profile but does not satisfactorily deskew the anomalies of any flank.

of wide anomalies, the two shoulders of the anomaly should reach the same amplitude; in the case of narrow anomalies, characterized by a single peak, both sides of the peak should display similar slopes.

The skewness factor can be determined visually [*Schouten and Cande,* 1976; *Cande,* 1976; *Petronotis and Gordon,* 1989]. We designed an interactive graphic computer program to approach, in a dichotomous way, the optimal skewness needed to make a magnetic anomaly symmetrical. Tests on synthetic magnetic anomalies show that this method reaches an accuracy of 1-2° for broad and tabular anomalies and 2-4° for narrow and peaked anomalies. Further tests on real data show that, for broad and tabular anomalies, the accuracy is about 1-2° for clean data and 2-4° for noisy data. Such a visual method may, however, be regarded as subjective, and semiautomated methods, based on mathematical criteria, have been designed to determine skewness [*LaBrecque,* 1973, 1976; *Arkani-Hamed,* 1991; *Roest et al.,* 1992].

LaBrecque [1973, 1976] proposed an iterative method based on the correlation, in the Fourier domain, of the magnetic anomaly with a boxlike magnetization function built from the magnetic anomaly itself such that it is equal to -1 for negative anomalies and +1 for positive anomalies. This method does not require, as erroneously stated by *Roest et al.* [1992], a priori knowledge of reversals and spreading rates. The correlation presents a linear trend across a range of frequency bands, and the intercept of this trend with the ordinate axis is used as a phase shift to apply to the anomaly. This process is iteratively repeated to the phase-shifted anomaly until the intercept becomes negligible, and the anomaly is deskewed. The sum of the successive phase shifts applied to the initial anomaly represents its skewness factor. Our implementation of this method makes the skewness determination a rather long process, as we choose to select interactively the range of frequencies used for the regression at every iteration to insure the convergence. The method provides accurate values of skewness for very clean anomaly data; however, it is inadequate for handling noisy data.

Arkani-Hamed [1991] designed a simple method to determine the skewness of a magnetic anomaly. He calculated correlation coefficients between the observed anomaly, gradually phase-shifted by increments of 2°, and the corresponding synthetic magnetic anomaly computed at the pole under the assumption of rectangular, two-dimensional prisms of constant magnetization and alternating polarity. The anomaly is deskewed for the phase shift which corresponds to the maximum correlation coefficient. This method was applied to synthetic magnetic anomalies computed from various magnetization models of oceanic lithosphere [*Arkani-Hamed,* 1989, 1991] and to five aeromagnetic profiles across anomaly 33r northeast of Newfoundland [*Arkani-Hamed,* 1990]. It has the advantage to allow skewness determination of a single anomaly. However, in the case of real data, it requires a precise determination of the spreading rate for each anomaly and an uncertain adjustment of the measured and synthetic profiles in order to make the correlation meaningful. Such requirements make the method time consuming and not suitable for investigation of a large set of data.

Roest et al. [1992] used a method based on the analytic signal, a complex function built from the magnetic anomaly derivatives as a pair of Hilbert transforms. The modulus of the analytic signal is independent of the magnetic anomaly skewness factor and reaches a maximum at the top of magnetic contrasts [*Nabighian,* 1972, 1974]. *Roest et al.* [1992] noted that for a deskewed magnetic anomaly, the horizontal derivative of the pseudo-gravity [*Cordell and Grauch,* 1985; *Blakely and Simpson,* 1986] computed from this anomaly is very similar to the modulus of the analytic signal. Correlation coefficients between the modulus of the analytic signal and the pseudo-gravity computed from the initial anomaly (gradually phase-shifted by increments of 1°) are computed. The anomaly is deskewed for the phase shift which corresponds to the maximum correlation coefficient. Our implementation of this method makes a skewness determination almost twice as fast as the visual method. We observe that *Roest et al.*'s [1992] method is less sensitive to noise than *LaBrecque*'s [1973, 1976] method but may produce aberrant results for noisy anomalies, particularly when the noise is local and does not equally affect the whole profile. Also the method is not suitable for narrow anomalies. Despite these shortcomings, we used both *Roest et al.*'s [1992] method and the visual method to independently determine the skewness of magnetic anomalies in the Indian Ocean.

Most of the previous analyses determined skewness for sets of anomalies rather than for each individual anomaly. They used data sets which were limited to the "best" profiles rather than all of the available data and/or performed the analysis for only selected anomalies. A detailed skewness analysis was conducted by *Petronotis and Gordon* [1989] in the northern Pacific Ocean. Following these authors, we analyze each individual anomaly along all the available profiles in the above-listed basins. About 250 magnetic profiles suitable for skewness analysis (Figure 1), almost parallel (within ±20°) to the spreading direction, are projected along this direction and resampled at an interval of 1 km; 1385 skewness measurements are made by the visual method and 782 by *Roest et al.*'s [1992] method. As we applied both methods to the same data set, we observe that *Roest et al.*'s [1992] method is unable to provide skewness determinations for more than one third of the cases for which the visual method works.

The measured skewness θ_m is defined by [*Schouten and McCamy,* 1972]

$$\theta_m = I'_r + I'_p - 180° + \theta_a \qquad (1)$$

where θ_a is the anomalous skewness, and I'_r and I'_p are the effective inclinations of the magnetization and geomagnetic field vectors, respectively. The effective inclination I' is related to the inclination I by [*Gay,* 1963]

$$\tan I' = \tan I / \sin(A - D) \qquad (2)$$

where A is the strike of the magnetic lineations measured 90° clockwise from the direction in which the seafloor becomes younger and D is the declination. I'_p is easily computed for a given latitude, longitude, and spreading direction from the International Geomagnetic Reference Field (IGRF) models [*IAGA Division V Working group 8,* 1992]. We define

$$I'_{ar} = I'_r + \theta_a = \theta_m - I'_p + 180° \quad (3)$$

as the apparent effective remanent inclination [*Petronotis et al.,* 1992], or AERI. AERI is computed for skewness determined by both the visual method and automated method of *Roest et al.* [1992]. When possible, AERI values corresponding to a given magnetic anomaly in a given basin are averaged and the standard deviation is computed in order to provide an error estimate.

Results for Conjugate Basins in the Indian Ocean

Figure 3 shows the resulting AERI for two pairs of conjugate basins versus age, using skewness determined by *Roest et al.*'s [1992] (top) and the visual (bottom) methods. Both methods provide similar results, indistinguishable at the level of uncertainty of our measurements (Figure 3). However, due to the difficulties of *Roest et al.*'s [1992] method in dealing with noisy data and narrow anomalies, the number of AERI obtained by this method is about one third less than that of the visual one. These "missing" AERI values correspond generally to the slower spreading rates, and their absence may induce a bias in the results (Figure 3). We only present results obtained by the visual method in this paper.

Figure 4 and Table A1[1] present AERI determined by the visual method versus age for the five pairs of conjugate basins considered in the Indian Ocean. The conjugate AERI curves shows the superposition of three effects: (1) the long-period (10-40 m.y.) trend of the average of conjugate AERI represents the paleomagnetic signature of ridge motions; (2) the intermediate-period (5-20 m.y.) difference between conjugate curves corresponds to the anomalous skewness senso stricto; and (3) the short-period (1-5 m.y.) difference between conjugate curves represents the effect of neighboring sources on a given anomaly, hereinafter called the sequence effect.

[1]An electronic supplement of this material may be obtained on a diskette or Anonymous FTP from KOSMOS.AGU.ORG. (LOGIN to AGU's FTP account using Anonymous as the username and GUEST as the password. Go to the right directory by typing CD APEND. Type LS to see what files are available. Type GET and the name of the file to get it. Finally, type EXIT to leave the system.) (Paper 94JB02061, Skewness of marine magnetic anomalies created between 85 and 40 Ma in the Indian Ocean, by J. Dyment, S.C. Cande, and J. Arkani-Hamed). Diskette may be ordered from American Geophysical Union, 2000 Florida Avenue, N.W., Washington, DC 20009; $15.00. Payment must accompany order.

Paleomagnetic Signature of Plate Motions

For all of the basins and during the period studied, the long-period trend of the average of conjugate AERI displays a gradual increase with time (Figure 4), representing the time variation of the effective inclination of the magnetization I'_r which corresponds to the effective paleoinclination of the magnetic field. Assuming that the magnetic field is dipolar, paleoinclinations I_r may be converted to paleolatitudes λ_r by

$$\tan I_r = 2 \tan \lambda_r. \quad (4)$$

If the azimuth of the ridges attached to the Indian plate did not drastically vary between 85 and 40 Ma, the gradual increase of AERI with time would reflect the northward motion of the ridges separating India (fastly moving northward) from Africa, Antarctica, and Australia (quasi-stationary or relatively slow in the geomagnetic reference frame). The azimuths of the ridges attached to India are poorly known for the period considered, and we are not able to determine the true paleoinclinations and compute the true paleolatitudes. Therefore effective paleolatitudes are obtained by averaging conjugate AERI, applying equation (4) with averaged AERI in place of I_r, and fitting a linear regression to remove the intermediate- and short-period effects.

Effective and true paleolatitudes are generally different, except for east-west trending ridges, as more or less verified for the ridges attached to the Indian plate according to paleogeographic reconstructions for chrons 34, 29, 24, and 21 which were plotted in the geomagnetic reference frame [*Besse and Courtillot,* 1988]. Indeed, our effective paleolatitudes are in rough agreement with Besse and Courtillot's paleolatitudes, differing by less than 15° (Table 1). The best agreement is observed for the Southeast Indian Ridge, with an orientation closer to the east-west direction. Figure 5 displays the observed effective paleolatitudes and the regression lines for the Indian Ocean ridges. The Central Indian Ridge appears to have been located south of the Southeast Indian Ridge, an artifact due to the different orientation of these ridges. Slopes of regression lines are 65 km/m.y. for the Southeast Indian Ridge and 50 km/m.y. for both the Carlsberg and Central Indian Ridges. These slopes can only be interpreted as velocities with respect to the geomagnetic reference frame if the ridge orientation remained constant during the period considered.

We also apply the lune intersection method [*Schouten and Cande,* 1976; *Cande,* 1976] to our data for anomalies 29, 24, and 21 on the Indian plate and compare the resulting zones of lune intersection to the apparent polar wander path for India [*Besse and Courtillot,* 1991]. The average AERIs of the selected anomaly in all pairs of conjugate basins are used, and a ±5° uncertainty is assigned to define the confidence lunes. The Mascarene Basin, however, was discarded because its northern flank, created on the Indian plate, now belongs to the African plate. The lunes of confidence (Figure 6) intersect in elongated zones, as the basins located on the Indian plate are rather close and display

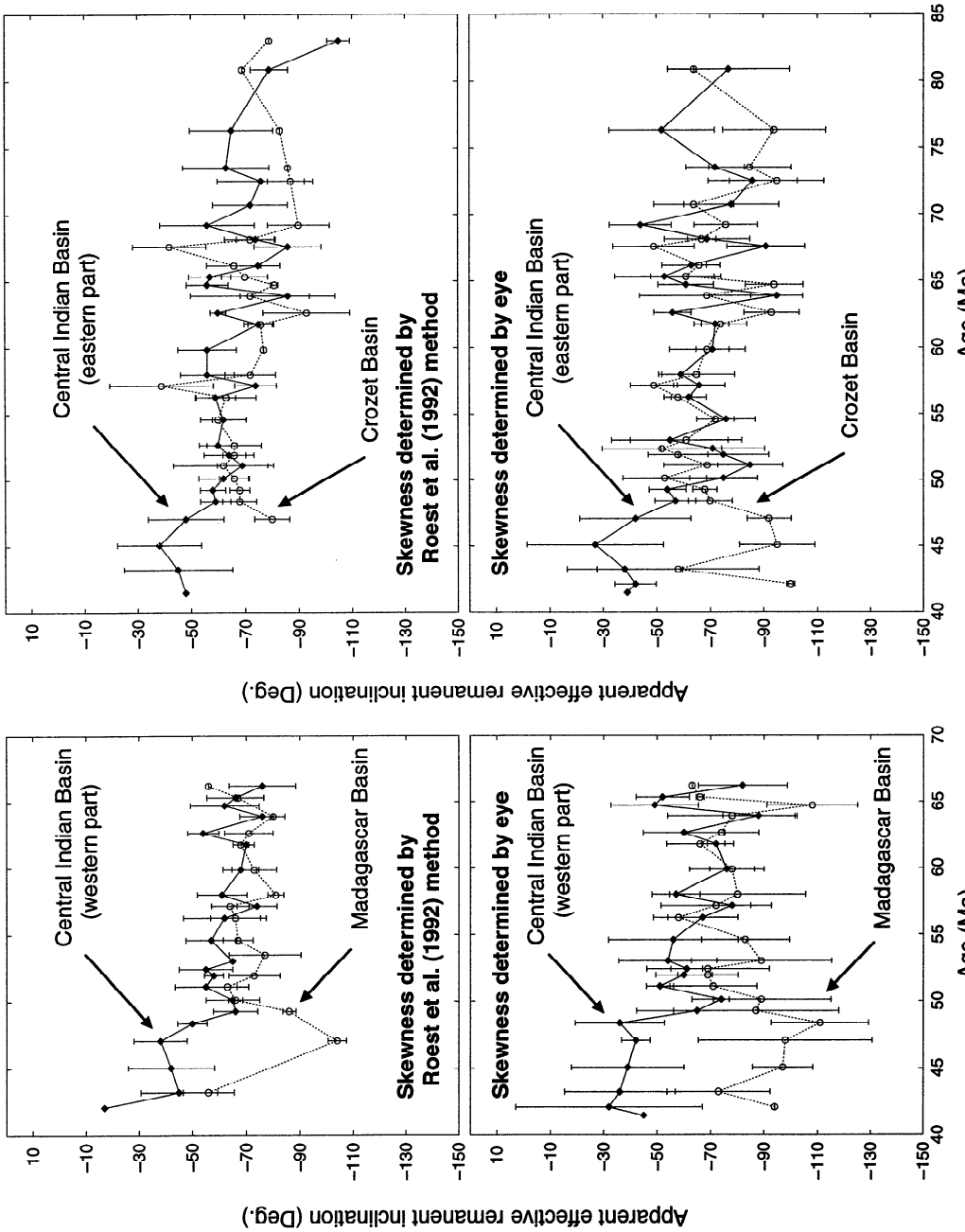

Figure 3. Apparent effective remanent inclination (i.e., skewness corrected for present geomagnetic field effective inclination) versus time for two pairs of conjugate basins. Solid diamonds and solid lines correspond to the northern basins; circles and dotted lines correspond to the southern basins. The error bars are standard deviations if more than one measurement is available. Top diagrams show results obtained by *Roest et al.*'s [1992] method; bottom diagrams show results obtained by the visual method.

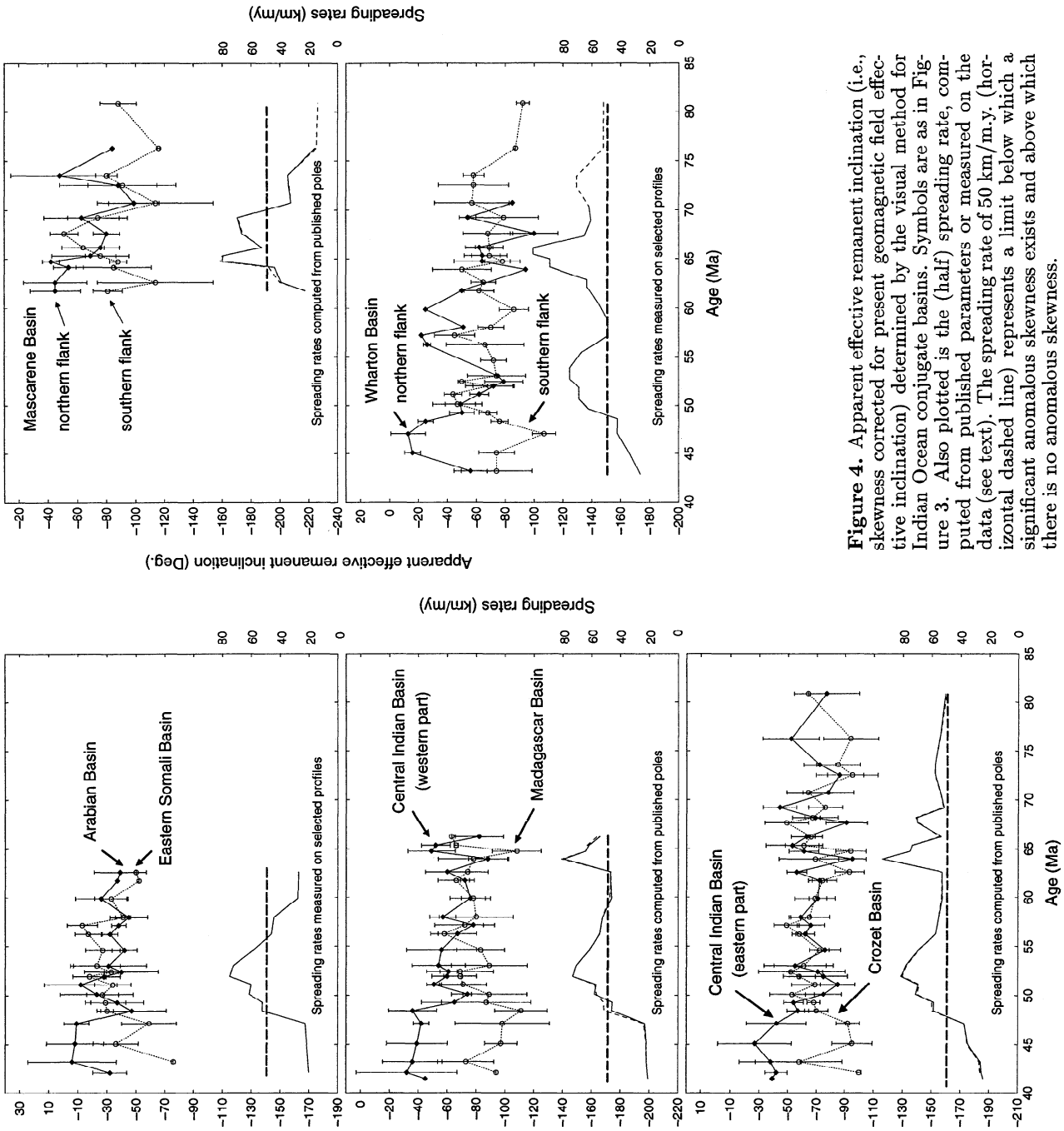

Figure 4. Apparent effective remanent inclination (i.e., skewness corrected for present geomagnetic field effective inclination) determined by the visual method for Indian Ocean conjugate basins. Symbols are as in Figure 3. Also plotted is the (half) spreading rate, computed from published parameters or measured on the data (see text). The spreading rate of 50 km/m.y. (horizontal dashed line) represents a limit below which a significant anomalous skewness exists and above which there is no anomalous skewness.

Table 1. Effective Paleolatitude and Paleolatitude of Indian Ocean Ridges

Chron	Age (Ma)	Carlsberg	CIR	SEIR	Wharton
21	≈ 47	-16 ± 5 (-12 ± 7)	-51 ± 15 (-37 ± 4)	-45 ± 15 (-43 ± 6)	-36 ± 15 (-26 ± 6)
24	≈ 53	-18 ± 5 (-15 ± 6)	-53 ± 12 (-41 ± 4)	-48 ± 15 (-47 ± 5)	-40 ± 20 (-30 ± 4)
29	≈ 65	...	-59 ± 12 (-49 ± 4)	-55 ± 15 (-56 ± 7)	-50 ± 20 (-40 ± 6)
34	≈ 83	...	...	-65 ± 20 (-58 ± 5)	...

Effective paleolatitudes are from marine magnetic anomaly skewness, in degrees, and paleolatitude (in parentheses) are from paleomagnetic measurements and paleogeographic reconstructions [*Besse and Courtillot,* 1988], in degrees.

similar anomaly trends. Using the intersection of three or four lunes, a good agreement with *Besse and Courtillot* [1991] poles for anomaly 29 and a fair agreement for anomalies 24 and 21 are observed.

Anomalous Skewness

The difference between conjugate AERI curves represents twice the anomalous skewness. For clarity, we separate anomalous skewness senso stricto, which represents the intermediate period (5-20 m.y.) component evidenced by previous workers, from the short-period combination of sequence effect and noise related to erroneous skewness measurements. Like *Cande* [1976] and *Cande and Kristoffersen* [1977], we assume that anomalous skewness is evenly distributed over conjugate basins. *Roest et al.* [1992] computed independent anomalous skewness estimates for both conjugate basins by using published or interpolated paleomagnetic poles to determine I'_r. While paleomagnetic poles are rather well constrained for the continents surrounding the Atlantic Ocean, they are scarce, unevenly distributed, and affected by large uncertainties for the continents surrounding the Indian Ocean. They are not used in this study. The assumption of evenly distributed anomalous skewness is supported by the measurements of *Roest et al.* [1992], which show only one uneven case for the Arctic Ocean, possibly due to the larger uncertainty on the paleo-azimuth of the high-latitude Nansen Ridge. Anomalous skewness is observed in the five pairs of conjugate basins considered in the Indian Ocean (Figure 4). It is evident for times younger than 50 Ma in the Arabian and Eastern Somali Basins, in the western Central Indian and Madagascar Basins, in the eastern Central Indian and Crozet Basins, and for both flanks of the Wharton Basin, and for times younger than 65 Ma in the Mascarene Basin. It is apparent before 70 Ma in the western Central Indian and Crozet Basins and for both flanks of the Mascarene Basin. It possibly existed in the Wharton Basin between 57 and 62 Ma.

A spreading rate dependence of anomalous skewness has been suspected since the discovery of anomalous skewness [*Cande,* 1976] and has clearly been established by *Roest et al.* [1992], who showed that anomalous skewness increases as spreading rate decreases. Figure 7 shows our observations of anomalous skewness plotted versus spreading rate and *Roest et al.*'s [1992] observations of anomalous skewness for anomalies 20 reversed (noted 20r), 25r, and 33r for comparison. There is a good agreement between our and *Roest et al.*'s [1992] anomalous skewness determinations. The large scatter of our measurements and the difference between *Roest et al.* [1992] curves are likely to be related to the sequence effect (see below). Both *Roest et al.*'s [1992] and our skewness determinations were performed on projected and regularly resampled magnetic anomaly data, without any additional processing. In particular, the data were not normalized to the same spreading rate, because (1) spreading rates vary along a profile and make the normalization complicated, (2) their determination depends on the geomagnetic polarity time scale used, which is subject to frequent changes [e.g., *Cande and Kent,* 1992], and (3) the normalization procedure proposed by *Schouten and McCamy* [1972] and *Cande* [1978] assumes rectangular, two-dimensional prisms of constant magnetization and alternating polarity, an assumption proven inadequate by the observation of anomalous skewness. *Cande* [1978] reported that the anomalous skewness of magnetic anomaly 33 and 34 in the South Atlantic changed by 10° after normalization from 30 to 15 km/m.y., and therefore one may argue that the observed relation between anomalous skewness and spreading rate is ficticious, reflecting the lack of normalization.

The spreading rate normalization is an operation which accounts for the different Earth filters generated by different spreading rates [*Schouten and McCamy,* 1972; *Cande,* 1978]. The Earth filter in the Fourier domain is [*Schouten and McCamy,* 1972]

$$E(u) = e^{-au} - e^{-bu} \tag{5}$$

where a and b are the depth to the top and bottom of the rectangular prisms from the observation plane and u is the wave number. Normalization to a given spreading rate is characterized in the Fourier domain by a filter

$$N = E(u_N)/E(u_O) \tag{6}$$

where u_O and u_N are the original and normalized wave numbers, related by

$$u_N V_N = u_O V_O \tag{7}$$

to the original and normalized spreading rates, V_O and V_N. In order to test the effect of spreading rate normalization, we measured the spreading rate and applied the normalization to every anomaly 27r recorded in the studied area. The spreading rates range from 25 to 70 km/m.y. We normalized the anomalies to a spreading rate of 35 km/m.y. and determined the anomalous skewness of normalized anomalies, to be compared with

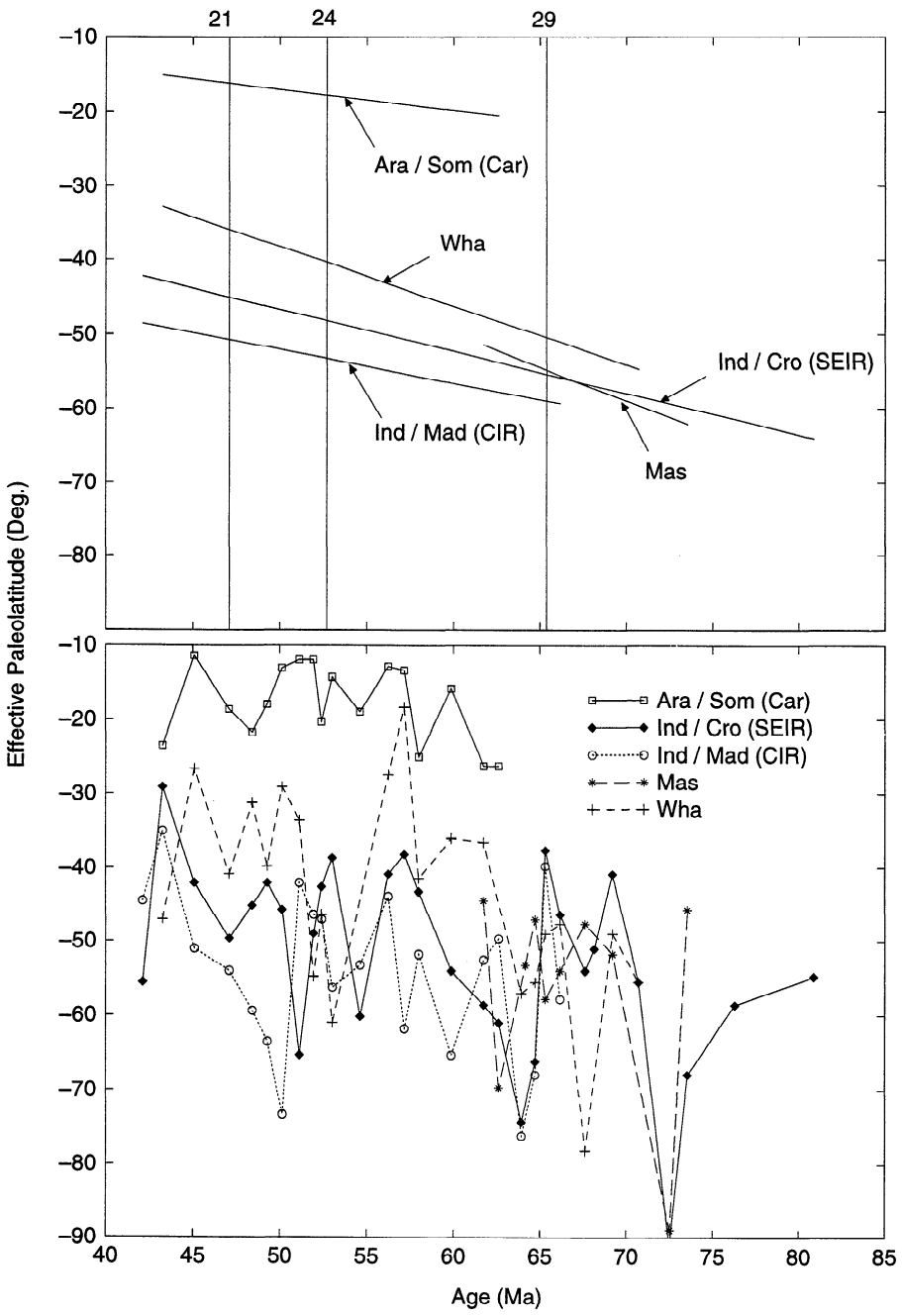

Figure 5. Effective paleolatitudes of the Indian Ocean ridges determined from apparent effective remanent inclinations (AERI) averaged over conjugate basins. See Figure 1 for abbreviations. Through relation (4), the uncertainty and noise on AERI increase for AERI higher than 55° (paleolatitudes higher than 35°) and decrease for AERI lower than 55° (paleolatitude lower than 35°), an effect responsible for larger scatter for the SEIR, CIR, and Wharton Basin than for the Carlsberg Ridge (bottom). For clarity, uncertainty bars are omitted. The typical 15° uncertainty on AERI induces uncertainties of 7°, 12°, 15°, and 25° on effective paleolatitude at the equator, 20°, 35°, and 60°, respectively. Despite this effect, the gradual trend of the effective paleolatitudes versus age (data, bottom, and linear regression, top) suggests that the ridge orientation remained relatively stable. The position of the Central Indian, Carlsberg, and Mascarene Ridges with respect to the Southeast Indian and Wharton Ridges is biased by their different orientation.

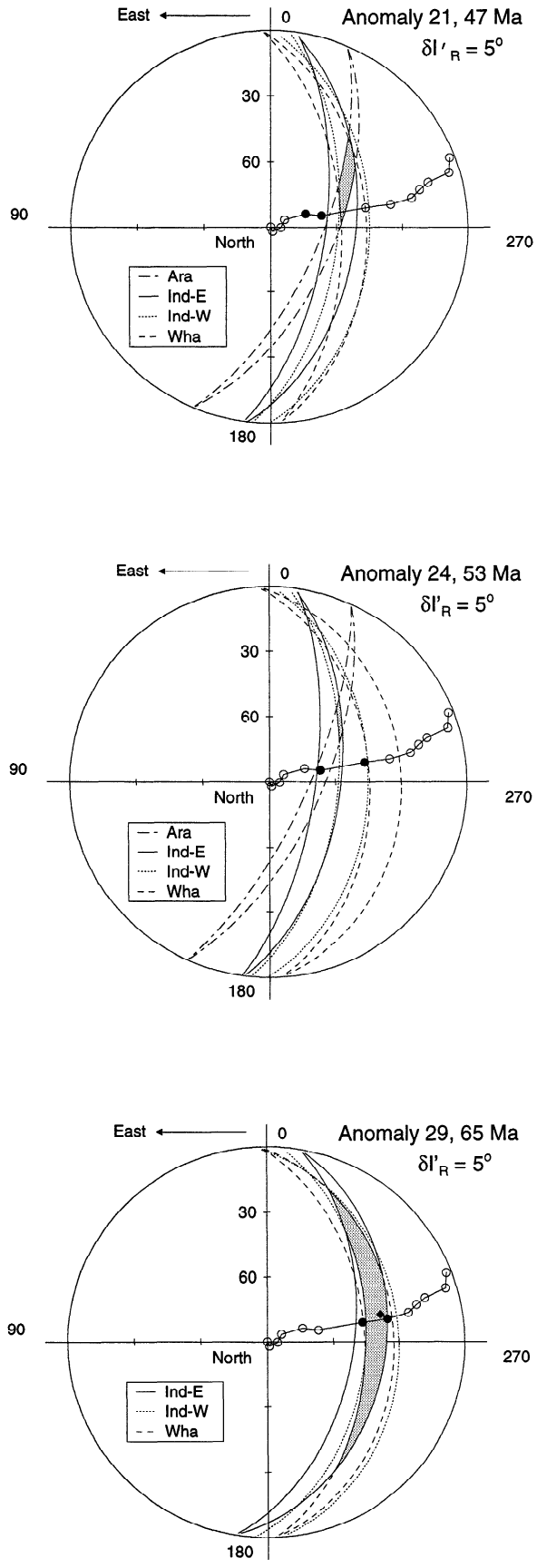

the anomalous skewness of the original anomalies. The normalization does not show any systematic effect on anomalous skewness with spreading rate. The difference is never larger than 10° and does not significantly affect *Roest et al.*'s [1992] and our results.

Although a diagram of anomalous skewness versus spreading rate reveals the general trend of their relationship (Figure 7), the short-period component obscures another important observation which can be made from conjugate AERI curves versus time (Figure 4). For example, the conjugate western Central Indian and Madagascar Basins display no significant anomalous skewness between 67 and 50 m.y. (the difference of conjugate AERI curves is limited to short-period fluctuations). On the contrary, they present a large anomalous skewness, about 30°, between 50 and 40 m.y. The transition corresponds to the well-known decrease of spreading rates observed in the Indian Ocean after the collision of India with Eurasia started [*Patriat and Achache,* 1984]. We note, however, that the transition between the two anomalous skewness periods is very short, less than 2 m.y. Similar observations can be made from the other basins (Figure 4). If the spreading rate dependence of anomalous skewness is gradual, as suggested by *Roest et al.* [1992, Figure 9], the short transition implies a spreading rate jump from 80-60 to 30-10 km/m.y. at 50 Ma. While spreading rate has in fact decreased from 70 to 20 km/m.y. on the Central Indian Ridge, this decrease is believed to have occurred over at least 7 m.y., from 54 to 47 Ma, and not in a period shorter than 2 m.y.

Included in Figure 4 is the spreading rate versus time for comparison with conjugate AERI curves. Spreading rates were computed from detailed rotation parameters (angles are adapted to the timescale of *Cande and Kent* [1992]) when available (Mascarene Basin [*Dyment,* 1991] and Central Indian, Crozet, and Madagascar Basins [*Patriat,* 1987]), or measured on the data and

Figure 6. (opposite) Paleomagnetic pole determinations for the Indian plate by the lune method [*Schouten and Cande,* 1976] for anomalies 21, 24, and 29. See Figure 1 for abbreviations. Effective paleoinclinations were obtained by averaging apparent effective remanent inclinations for conjugate basins. Effective inclinations from the Mascarene Basin were discarded, as this basin belongs to the African plate since anomaly 27 [*Dyment,* 1991]. The intersection of three or four almost parallel lunes of confidence is shaded. The apparent polar wander (APW) path for India proposed by *Besse and Courtillot* [1991] is shown by circles (every 10 m.y., from present at the north pole back to 120 m.y.) and solid line. The solid circles indicate the section of the APW path corresponding to the given anomaly: 40-50 Ma for anomaly 21, 50-60 Ma for anomaly 24, and 60-70 Ma for anomaly 29. The A_{95} confidence circles on these paleomagnetic poles, omitted for clarity, are 4.8° at 40 Ma, 6.0° at 50 Ma, 8.9° at 60 Ma and 6.3° at 70 Ma [*Besse and Courtillot,* 1991]. The diamond for anomaly 29 represents paleomagnetic measurement from the Deccan Traps, with an A_{95} confidence circle of 2° [*Besse and Courtillot,* 1988 and 1991].

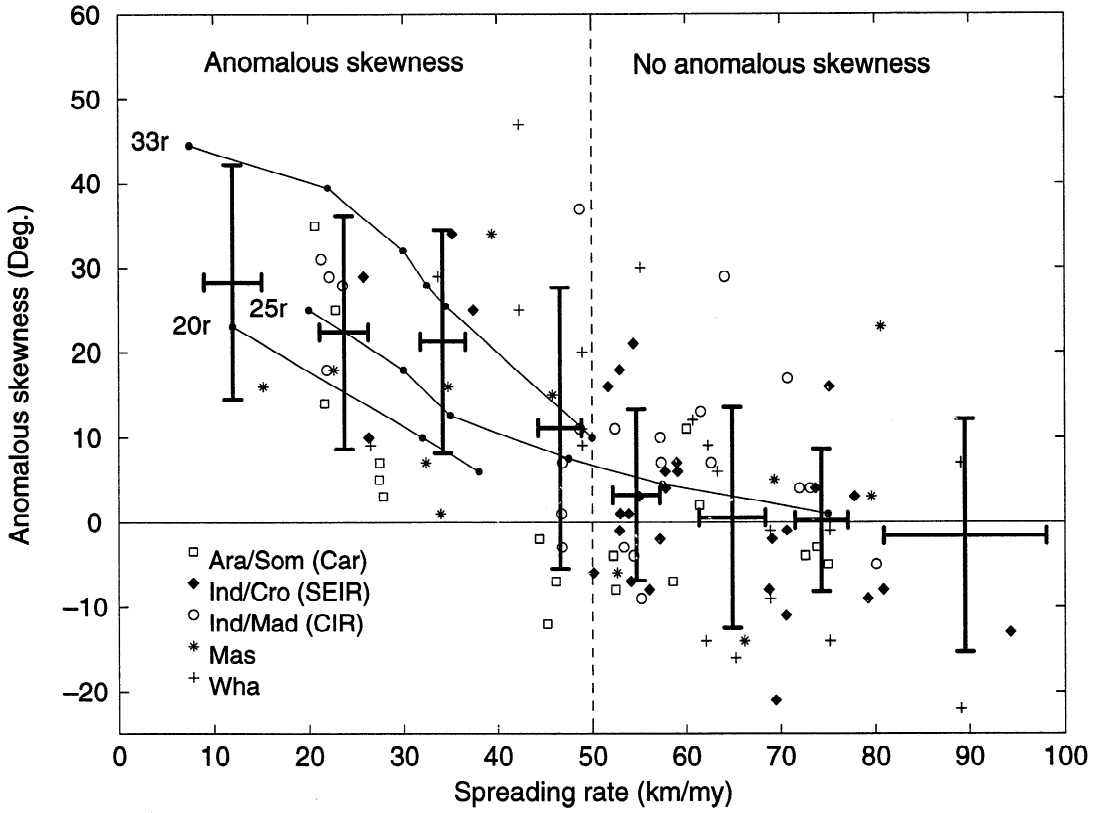

Figure 7. Anomalous skewness (i.e., half difference between apparent effective remanent inclination of conjugate basins) versus spreading rate for all studied basins. See Figure 1 for abbreviations. Despite a large dispersion related to the sequence effect and errors in skewness determination, anomalous skewness decreases with increasing spreading rate. This observation is in agreement with *Roest et al.*'s [1992] results, displayed for comparison (curves labeled 33r, 25r, and 20r). Averages and standard deviations of available anomalous skewness determinations [*Roest et al.*, 1992; this study] within 10 km/m.y. intervals (20 km/m.y intervals below 20 km/m.y. and above 80 km/m.y.) are represented by bold uncertainty bars. There is a limit at a spreading rate of 50 km/m.y. (dashed line), below which anomalous skewness is observed and above which there is no significant anomalous skewness.

computed using the *Cande and Kent* [1992] geomagnetic polarity timescale (Arabian, Eastern Somali, and Wharton Basins). A comparison of anomalous skewness and spreading rate versus time confirms the relation between slow (respectively fast) spreading rate and high (respectively low or null) anomalous skewness (Figure 4). It also shows that the transition between periods of significant anomalous skewness and almost no anomalous skewness corresponds to a spreading rate of about 50 km/m.y. half rate.

Sequence Effect

Petronotis and Gordon [1989] observed short-period fluctuations on the AERI curve of the North Pacific basin. They noted some differences between positive and negative anomalies but did not attempt to explain this observation, because subduction has destroyed the conjugate basin. They considered the short-period fluctuations as noise. The short-period (1-5 m.y.) fluctuations of the Indian Ocean AERI curves (Figure 4) are not randomly distributed, rather they appear opposite in sign for conjugate basins, although the observation is not systematic because noise accounts for a significant part of the short-period component. The conjugate AERI curves from the western Central Indian and Madagascar Basins, and the eastern Central Indian and Crozet Basins, respectively, are particularly convincing (Figure 4). We propose that the opposite fluctuations represent the effect of the source of neighboring anomalies on the studied anomaly, and call it the sequence effect. This effect is inherent in the definition of a deskewed magnetic anomaly used with the visual method, i.e., a symmetrical anomaly (see discussion above). We note that *Roest et al.*'s [1992] method, which is based on another criterion, tends to reduce, but does not remove, the sequence effect (Figure 3).

The sequence effect is observed in all pairs of conjugate basins we considered. In order to determine if similar patterns are observed from one basin to another, we isolated the short-period fluctuations by removing a linear trend from AERI curves and inverting those from the southern basins (Figure 8). Although the

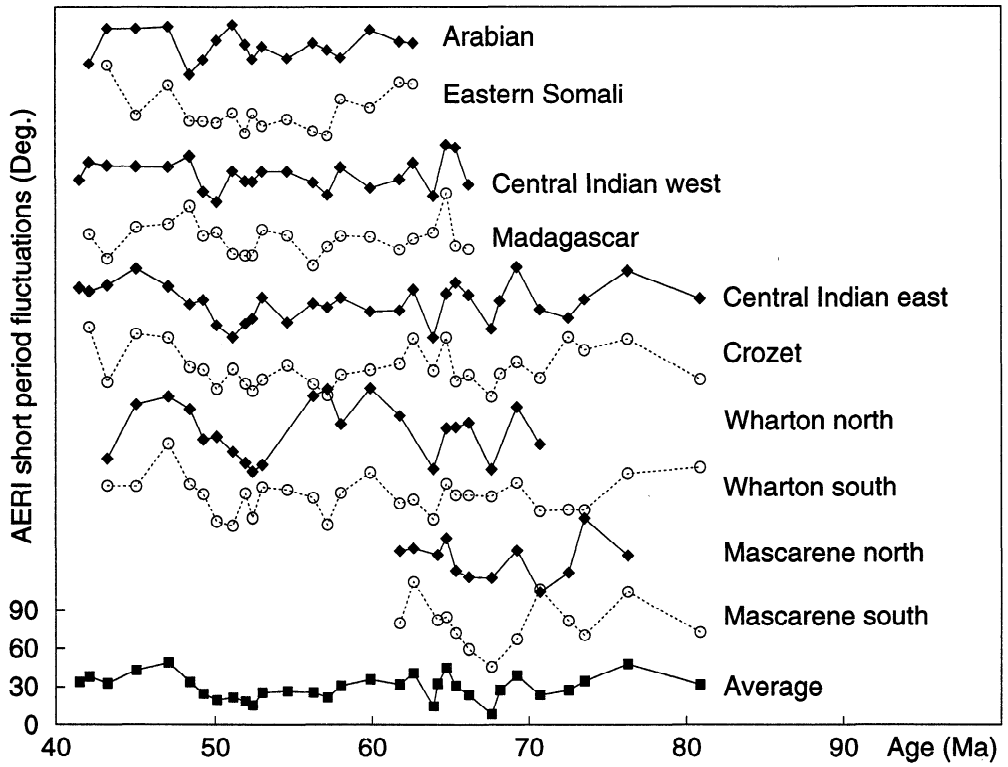

Figure 8. Short-period fluctuations of apparent effective remanent inclination: a linear trend is removed for all basins, and curves are inverted for southern basins (open circles and dotted lines) only. The non-null average (bottom) reveals fluctuations which are common to several pairs of conjugate basins, especially between 63 and 71 Ma (anomalies 28 to 31r).

linear trend is not accurate to correct the long-period effects, and some curves show obvious contamination from anomalous skewness, this rough processing is sufficient enough to recognize similar short-period fluctuations between 63 and 71 Ma (anomalies 28 to 31r) for at least six short-period curves (Figure 8). The average of AERI short-period fluctuations, also displayed on Figure 8, has significant amplitudes, particularly between 63 and 71 Ma. If the short-period fluctuations only reflect random errors on the skewness measurements, their average should be close to zero.

Although widely observed, the sequence effect may have different expressions for different pairs of conjugate basins, as it is expected to vary with spreading rate. The effect of neighboring anomalies depends on the distance and therefore on the spreading rate as well as on the temporal sequence of positive and negative geomagnetic polarity intervals. For polarity intervals of approximately the same duration, fast spreading rates tend to separate the sources responsible for the anomalies and therefore result in smaller sequence effects. For a more complex sequence of short and long polarity intervals, however, the combination of spreading rate and temporal sequence can make the sequence effect unpredictible. As an example, synthetic anomalies 27-31 were computed at the pole for several spreading rates, under the assumption of rectangular, two-dimensional prisms of constant magnetization and alternating polarity (Figure 9). The sequence effect is important for anomalies 26r, 27r, 28, 29, 30, and 31, in agreement with our observations (Figure 8). Due to the brevity of anomaly 30r, anomalies 30-31 may be considered as a single anomaly at slow spreading rates and two separate anomalies at fast spreading rates. The sequence effect associated with anomalies 30-31, taken together, displays a complex evolution with spreading rate. In addition, we note that the sequence effect varies if another source model (i.e., different source geometry, type of magnetization and/or geomagnetic field behavior) is adopted.

Summary and Conclusions

The skewness of marine magnetic anomalies in the Indian Ocean obtained by the visual method [e.g., *Cande*, 1976] and the analytic signal method [*Roest et al.*, 1992] is remarkably similar and can be interpreted as the superposition of three effects: a gradual increase of apparent effective remanent inclination with time, due to the northward motion of ridges attached to the Indian plate; the anomalous skewness; and short-period fluctuations representing the effect of neighboring sources on the skewness of a given anomaly. The anomalous skewness decreases with faster spreading rate and becomes negligible above 50 km/m.y.

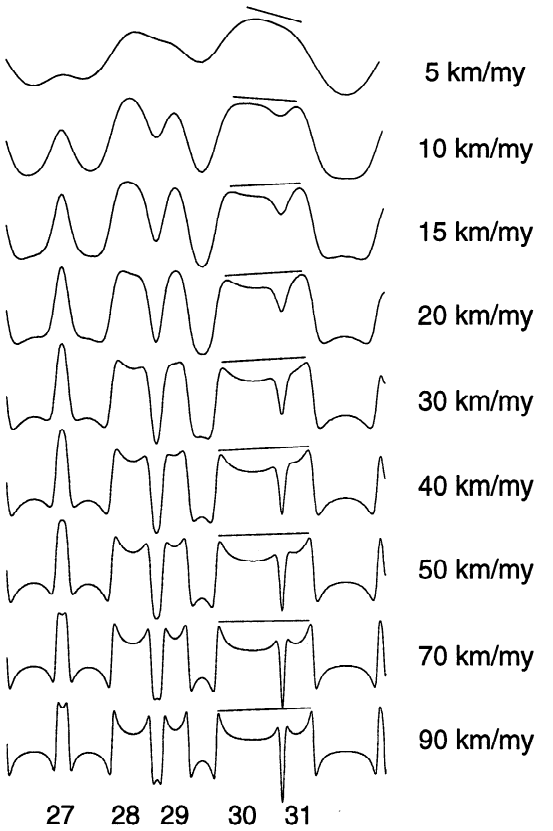

Figure 9. Synthetic marine magnetic anomalies 27-31 computed at the pole for several spreading rates, under the assumption of rectangular, two-dimensional prisms of constant magnetization and alternating polarity. Important sequence effect is observed for anomalies 26r (26 reversed), 27r, 28, 29, 30 and 31, in agreement with observations (Figure 8). Due to the brievity of anomaly 30r, anomalies 30-31 may be considered as a single anomaly for slow spreading rates and two separates anomalies at fast spreading rates. The sequence effect associated with anomalies 30-31 taken together displays a complex evolution with spreading rate, emphasized by the varying slope of the line segments over the anomalies.

The latter observation has important implications on the cause of anomalous skewness. Two classes of models have been proposed to explain the anomalous skewness of marine magnetic anomalies: the first relies on systematic variations of the geomagnetic field intensity within each polarity interval [*Cande,* 1978], and the second considers that seafloor spreading processes cause the magnetic properties of the oceanic lithosphere to depart significantly from the standard uniformly magnetized rectangular prism model [*Cande,* 1978; *Cande and Kent,* 1978; *Verosub and Moores,* 1981; *Raymond and LaBrecque,* 1987; *Arkani-Hamed,* 1989]. Obviously no geomagnetic field behavior can predict the observation, for the same time interval, of a significant anomalous skewness at slow spreading centers and no anomalous skewness at fast spreading centers: the spreading rate dependence of the anomalous skewness clearly points toward seafloor spreading processes as the major cause of anomalous skewness. Variations of the thermal, tectonic, and chemical parameters of accretionary processes with spreading rates [e.g., *Chen and Morgan,* 1990; *Phipps Morgan and Chen,* 1993; *Sinton and Detrick,* 1992; *Niu and Batiza,* 1993] likely result in a spreading rate dependent magnetization of the different oceanic layers, which may be responsible for the observed anomalous skewness. Determination of the dominant effects and their modeling is beyond the scope of this paper and is the subject of ongoing investigations.

Acknowledgments. This work was initiated when J.D., then funded by the French Ministry of Education (AER contract) and Société de Secours des Amis des Sciences at Ecole et Observatoire de Physique du Globe de Strasbourg, was visiting Lamont-Doherty Geological Observatory for 6 months as post-doc. It was later continued at McGill University with the attribution of an International Fellowship by the Natural Science and Engineering Research Council (NSERC) of Canada to J.D. J.A.H. was funded by NSERC operating grant OGP0041245. We thank the members of the "Alliance Exotique" (Indian Ocean Data Compilation Project, principal investigators R. Schlich, J.G. Sclater, R.L. Fisher, S.C. Cande, M.F. Coffin, and H. Bergh) for providing the magnetic data. We acknowledge valuable discussions with J.L. LaBrecque. We also thank R.D. Mueller, W.R. Roest, J.Y. Royer, L.M. Gahagan, and J.G. Sclater for the digital World's Oceans age map used to produce Figure 1, P. Wessel and W.H.F. Smith for the GMT software used to produce Figure 1, and P.J. Turner for the Xmgr software used to produce the other figures. Extensive reviews by Carol Raymond, Katerina Petronotis, and Doug Wilson improved the paper and are gratefully acknowledged.

References

Arkani-Hamed, J., Thermoviscous remanent magnetization of oceanic lithosphere inferred from its thermal evolution, *J. Geophys. Res., 94,* 17,421-17,436, 1989.

Arkani-Hamed, J., Magnetization of the oceanic crust beneath the Labrador Sea, *J. Geophys. Res., 95,* 7101-7110, 1990.

Arkani-Hamed, J., Thermoremanent magnetization of the oceanic lithosphere inferred from a thermal evolution model: Implications for the source of marine magnetic anomalies, *Tectonophysics, 192,* 81-96, 1991.

Besse, J., and V. Courtillot, Paleogeographic maps of the continents bordering the Indian Ocean since the early jurassic, *J. Geophys. Res., 93,* 11,791-11,808, 1988.

Besse, J., and V. Courtillot, Revised and synthetic apparent polar wander paths of the African, Eurasian, North American and Indian plates, and true polar wander since 200 Ma, *J. Geophys. Res., 96,* 4029-4050, 1991.

Blakely, R.J., and R.W. Simpson, Approximating edges of source bodies from magnetic or gravity anomalies, *Geophysics, 51,* 1494-1498, 1986.

Briais, A., P. Patriat, and P. Tapponnier, Updated interpretation of magnetic anomalies and seafloor spreading stages in the South China Sea: Implications for the Tertiary tectonics of Southeast Asia, *J. Geophys. Res., 98,* 6299-6328, 1993.

Cande, S.C., A palaeomagnetic pole from Late Cretaceous marine magnetic anomalies in the Pacific, *Geophys. J. R. Astron. Soc., 44,* 547-566, 1976.

Cande, S.C., Anomalous behavior of the paleomagnetic field inferred from the skewness of anomalies 33 and 34, *Earth Planet. Sci. Lett., 40,* 275-286, 1978.

Cande, S.C., and D.V. Kent, Constraints imposed by the shape of marine magnetic anomalies on the magnetic source, *J. Geophys. Res., 81,* 4157-4162, 1976.

Cande, S.C., and D.V. Kent, A new geomagnetic polarity time scale for the late Cretaceous and Cenozoic, *J. Geophys. Res., 97,* 13,917-13,951, 1992.

Cande, S.C., and Y. Kristoffersen, Late Cretaceous magnetic anomalies in the North Atlantic, *Earth Planet. Sci. Lett., 35,* 215-224, 1977.

Chen, Y.J., and W.J. Morgan, Rift valley/no rift valley transition at mid-ocean ridges, *J. Geophys. Res., 95,* 17,571-17,542, 1990.

Cochran, J.R., Somali Basin, Chain Ridge, and the origin of the Northern Somali Basin gravity and geoid low, *J. Geophys. Res., 93,* 11,985-12,008, 1988.

Cordell, L., and V.J.S. Grauch, Mapping basement magnetization zones from aeromagnetic data in the San Juan Basin, New Mexico, in *The Utility of Regional Gravity and Magnetic Anomaly Maps,* edited by W.J. Hinze, pp. 181-197, Society for Exploration Geophysicists, Tulsa, Okla., 1985.

Dyment, J., Structure et évolution de la lithosphère océanique dans l'océan Indien: Apport des anomalies magnétiques, Thèse doct., 374 pp., Univ. Pasteur, Strasbourg, France, 1991.

Gay, S.P., Standard curves for interpretation of magnetic anomalies over long tabular bodies, *Geophysics, 28,* 161-200, 1963.

Hilde, T.C.W., and C.S. Lee, Origin and evolution of the West Philippines Basin: a new interpretation, *Tectonophysics, 102,* 85-104, 1984.

IAGA Division V Working Group 8, IGRF, 1991 revision, *EoS Trans. AGU, 73,* 182, 1992.

LaBrecque, J.L., An accurate method of determining skewness (abstract), *EoS Trans. AGU, 54,* 252, 1973.

LaBrecque, J.L., A study of the marine magnetic anomaly pattern employing techniques based on the fast Fourier transform algorithm, Ph.D. thesis, 273 pp., Columbia Univ., New York, 1976.

LaBrecque, J.L., and D.E. Hayes, Seafloor spreading history of the Agulhas Basin, *Earth Planet. Sci. Lett., 45,* 411-428, 1979.

McKenzie, D.P., and J.G. Sclater, The evolution of the Indian Ocean since the Late Cretaceous, *Geophys. J. R. Astron. Soc., 25,* 437-528, 1971.

Nabighian, M.N., The analytic signal of two-dimensional magnetic bodies with polygonal cross-section: Its properties and use for automated anomaly interpretation, *Geophysics, 37,* 507-517, 1972.

Nabighian, M.N., Additional comments on the analytic signal of two-dimensional magnetic bodies with polygonal cross-section, *Geophysics, 39,* 85-92, 1974.

Niu, Y., and R. Batiza, Chemical variation trends at fast and slow spreading mid-ocean ridges, *J. Geophys. Res., 98,* 7887-7902, 1993.

Patriat, P., *Reconstitution de l'Evolution dy Système de Dorsales de l'Océan Indien par les Méthodes de la Cinématique des Plaques,* 308 pp., Territoire des Terres Australes et Antarctiques Françaises, Mission de Recherche, Paris, 1987.

Patriat, P., and J. Achache, India-Eurasia collision chronology has implications for crustal shortening and driving mechanism of plates, *Nature, 311,* 615-621, 1984.

Petronotis, K.E., and R.G. Gordon, Age dependence of skewness of magnetic anomalies above seafloor formed at the Pacific-Kula spreading center, *Geophys. Res. Lett., 16,* 315-318, 1989.

Petronotis, K.E., R.G. Gordon, and G.D. Acton, Determining palaeomagnetic poles and anomalous skewness from marine magnetic anomaly skewness data from a single plate, *Geophys. J. Int., 109,* 209-224, 1992.

Phipps Morgan, J., and Y.J. Chen, The genesis of oceanic crust: magma injection, hydrothermal circulation, and crustal flow, *J. Geophys. Res. 98,* 6283-6297, 1993.

Raymond, C.A., and J.L. LaBrecque, Magnetization of the oceanic crust: Thermoremanent magnetization or chemical remanent magnetization? *J. Geophys. Res., 92,* 8077-8088, 1987.

Roest, W.R., J. Arkani-Hamed, and J. Verhoef, The seafloor spreading rate dependence of the anomalous skewness of marine magnetic anomalies, *Geophys. J. Int., 109,* 653-669, 1992.

Schlich, R., The Indian Ocean: aseismic ridges, spreading centres and oceanic basins, in *Ocean Basins and Margins,* vol. 6, The Indian Ocean, edited by A.E.M. Nairn and F.G. Stehli, pp. 51-147, Plenum, New York, 1982.

Schlich, R., J.Y. Royer, H. Whitechurch, and M. Denis-Clocchiatti, Proposal for oceanic drilling at fossil ridges in the Indian Ocean, in *French Proposals for Oceanic Drilling in the Indian and Southern Oceans,* edited by R. Schlich and M. Munschy, ODP France, Strasbourg, France, 1985.

Schouten, H., and S.C. Cande, Palaeomagnetic poles from marine magnetic anomalies, *Geophys. J. R. Astron. Soc., 44,* 567-575, 1976.

Schouten, H., and K. McCamy, Filtering magnetic anomalies, *J. Geophys. Res., 77,* 7089- 7099, 1972.

Sinton, J.M., and R.S. Detrick, Mid-ocean ridge magma chambers, *J. Geophys. Res., 97,* 197- 216, 1992.

Srivastava, S.P., Evolution of the Labrador Sea and its bearing on the early evolution of the North Atlantic, *Geophys. J. R. Astron. Soc., 52,* 313-357, 1978.

Talwani, M., and O. Eldholm, Evolution of the Norwegian-Greenland Sea, *Geol. Soc. America Bull., 88,* 969-999, 1977.

Verosub, K.L., and E.M. Moores, Tectonic rotations in extensional regimes and their paleomagnetic consequences for ocean basalts, *J. Geophys. Res., 86,* 6335-6349, 1981.

Watts, A.B., J.K. Weissel, and R.L. Larson, Seafloor spreading in marginal basins of the western Pacific, *Tectonophysics, 37,* 167-181, 1977.

Weissel, J.K., and D.E. Hayes, Magnetic anomalies in the southeast Indian Ocean, in *Antarctic Oceanology II: The Australian-New Zeland Sector, Antarctic Res. Ser.,* vol. 19, edited by D.E. Hayes, pp. 165-196, AGU, Washington, D.C., 1972.

J. Arkani-Hamed, Earth and Planetary Sciences, McGill University, 3450 University St., Montréal, QC H3A-2A7, Canada. (e-mail: jafar@planet.eps.mcgill.ca)

S. C. Cande, Geological Research Division, Scripps Institution of Oceanography, La Jolla, CA 92093-0215. (e-mail: cande@gauss.ucsd.edu)

J. Dyment, URA 1278 et GDR GEDO, Université de Bretagne Occidentale, BP 809, 6 Avenue Le Gorgeu, 29285 Brest Cedex, France. (e-mail: jerome@univ-brest.fr)

(Received November 23, 1993; revised August 3, 1994; accepted August 11, 1994.)